MOLECULAR PHYSICS, 1981, VOL. 44, NO. 4, 849–869

Molecular dynamics of a model anisotropic system

by C. ZANNONI
Istituto di Chimica Organica, Universita', Viale Risorgimento 4, 40136 Bologna, Italy
and M. GUERRA
Laboratorio C.N.R. dei Composti del Carbonio contenenti Eteroatomi e loro Applicazioni, 40064 Ozzano Emilia, Italy

(*Received* 9 *February* 1981 ; *accepted* 4 *May* 1981)

The molecular dynamics method has been used to study a model system of 1000 symmetric top particles placed at the sites of a cubic lattice and interacting with the pair potential $U_{ij} = -\epsilon_{ij} P_2(\cos \beta_{ij})$. Here ϵ_{ij} is a positive constant, ϵ, for neighbouring sites and zero otherwise. The equations of motion are written in the quaternion representation and contact is made with the more familiar Euler parameterization of rotations. In particular, explicit expressions are given for the Wigner rotation matrices in terms of quaternions. The model is known from Monte Carlo simulations to possess an orientational phase transition and this fact is confirmed. Both static and dynamic properties have been calculated for a few selected temperatures. The singlet orientational distribution function has been obtained as a two dimensional histogram and order parameters $\langle P_2 \rangle$, $\langle P_4 \rangle$, $\langle P_6 \rangle$, have been calculated. It is shown that the appropriate way to describe the orientational dynamics in uniaxial systems of cylindrically symmetric particles is through the set of Wigner rotation matrix correlation functions $\phi_{mn}^{LL'}(t) = \langle D_{mn}^{L}(0)^* D_{mn}^{L'}(t) \rangle$. Results for the $\phi_{mn}^{LL'}(t)$ of ranks L, $L' = 1, 2$ are reported for two temperatures in the ordered phase and one in the isotropic phase. It is pointed out that correlation functions such as $\langle P_1(\mathbf{l}(0) \cdot \mathbf{l}(t)) \rangle$ and $\langle P_2(\mathbf{l}(0) \cdot \mathbf{l}(t)) \rangle$ depending solely on the angles between successive positions of the orientation vector $\mathbf{l}(t)$ only afford partial information on the dynamics, in contrast to the behaviour in isotropic systems. Although the model potential studied here is relatively simple the treatment is general and should be of use to future molecular dynamics simulations of anisotropic fluids.

1. INTRODUCTION

Computer simulations have contributed a great deal to our present insight of isotropic liquids [1, 2]. The impact of computer simulations on our understanding of anisotropic systems such as liquid crystals has been much smaller although reports of a few simulations have recently appeared [3–8]. The reasons for this situation are not difficult to understand. Liquid crystalline systems are extremely complex being composed of relatively large organic molecules [9]. This complexity rules out at present the possibility of realistic simulations such as those performed on simple fluids and molten salts [1, 2]. There is in fact no realistic intermolecular potential available for nematogenic molecules and even if such potentials were available the resulting simulation would probably be too

0026-8976/81/4404 0849 $02·00

complicated for the capabilities of present computers. In any case the first thing to attempt, before embarking on any extensive calculation, should be that of developing suitable algorithms for the computation of the relevant observables for the system. This is particularly true for models of liquid crystals because of the special problems connected with the existence of preferred directions in space. The definition and determination of the orientational phase transition itself, that is of the main characteristic of liquid crystals, requires considerable care [3, 5]. The same is true for the definition and calculation of single and pair distribution functions describing the ordering in an anisotropic system [10]. While some of these problems have already been dealt with or at least attacked in Monte Carlo investigations of nematic models a systematic approach to molecular dynamics simulation of anisotropic systems is still lacking. This seems a particularly severe limitation since it clearly leaves out the important reorientational properties of liquid crystals. We think it is important therefore to start by studying in detail some simple idealized model system which still contains the basic physics of the problem. Since we intend to concentrate on the most characteristic properties of liquid crystals, i.e. on orientational properties, a natural candidate seems to be the lattice model already studied by Lebwohl and Lasher [3 (b)] and various other workers using the Monte Carlo method [3–5] as well as approximate theoretical techniques such as mean field and two site cluster or others [11]. In the spirit of this investigation we shall discuss problems concerning molecular dynamics simulations of liquid crystals as generally as possible within the context of our model.

2. The model and its simulation

We describe only very briefly the lattice model employed since it is extensively discussed elsewhere [5]. It consists of a system of cylindrically symmetric particles or rather interaction centres located at the sites of a simple cubic lattice. The particles interact through a pair potential

$$U_{ij} = -\epsilon_{ij} P_2(\cos \beta_{ij}), \tag{1}$$

where ϵ_{ij} is a positive constant, ϵ, for neighbouring sites i and j and zero otherwise. The angle β_{ij} gives the relative orientation of particles i and j. The orientation of every particle can be written in general in terms of three Euler angles $(\alpha\beta\gamma)$ [12] transforming the laboratory fixed frame into a molecule fixed frame. We generalize slightly the model assuming that every particle is a symmetric top rotor. Thus it is natural to assume as molecule fixed coordinate system the principal axis system of the inertia tensor. This also defines the long molecular axis.

For a system of symmetric top particles the equations of motion for every particle can be written in terms of Euler angles [5] as

$$\ddot{\alpha} = \{(B-A)\dot{\alpha}\dot{\beta} \cos \beta \sin \beta + (A+B)\dot{\beta}\dot{\gamma} \sin \beta + N_\alpha - N_\gamma \cos \beta\}/A \sin^2 \beta, \tag{2a}$$

$$\ddot{\beta} = \{-(A+B)\dot{\alpha}\dot{\gamma} \sin \beta - B\dot{\alpha}^2 \sin \beta \cos \beta + N_\beta\}/A, \tag{2b}$$

$$\ddot{\gamma} = \{-(A+B)^2 \dot{\beta}\dot{\gamma} \cos \beta \sin \beta + (A - B \cos^2 \beta)(A+B)\dot{\alpha}\dot{\beta} \sin \beta + (A + B \cos^2 \beta)N_\gamma - (A+B) \cos \beta N_\alpha\}/A(A+B) \sin^2 \beta. \tag{2c}$$

Here $A = I_\perp$ and $B = I_\parallel - I_\perp$ where $I_\parallel$, $I_\perp$ are the principal components of the inertia tensor for the rotor. The quantities N_α, N_β, N_γ represent Euler

components of the torque **N** produced on the rotor under consideration by all the others in the system. In the molecular dynamics procedure new angles $(\alpha\beta\gamma)$ can be calculated from a knowledge of the old ones and the torques through integration of equations (2 *a*)–(2 *c*). However it is apparent that equations 2 lead easily to numerical problems. Thus it is seen that the sin β factor in the denominator causes the calculation to blow up every time β approaches zero. This is a well known problem in molecular dynamics simulation of systems of particles interacting via an angular dependent potential and various solutions have been suggested [7 (c), 13, 14].

In a preliminary set of calculations [5] we have used one such method, suggested by Barojas *et al.* [13]. It consists of continuously monitoring the value of every angle and switching to a different auxiliary laboratory system when β approaches zero. Evolution is then followed in the new laboratory system and the new calculated angles are subsequently transformed back to the original coordinate frame. The method obviously works but, apart from being inelegant it is rather time consuming and at least in our case leads to non-conservation of energy of the order of 1 per cent in a run of about five thousand time steps.

In the present set of calculations we followed therefore the suggestion by Evans [14] to parameterize orientations in terms of quaternions. Thus instead of three Euler angles $(\alpha\beta\gamma)$ we have four parameters u_0, u_1, u_2, u_3 linked by

$$u_0^2+u_1^2+u_2^2+u_3^2=1. \tag{3}$$

It is apparent that equation (3) is the equation of a sphere in a four dimensional space. The orientation of a rigid body of any shape is represented by a point on this hypersphere. Similarly the reorientation of the body corresponds to a trajectory on the surface of this sphere. In the special case of a linear molecule, a particle can be described in terms of two Euler or polar angles or alternatively in terms of three direction cosines. Its orientation can be described as a point on a three dimensional sphere of unit radius and its reorientation as a trajectory on the sphere. A similar representation can obviously be given, *a posteriori*, for the symmetry axis of a symmetric top particle. We show explicitly some typical trajectories for our system in the next section. From the point of view of simulations the main advantage of quaternions is that they eliminate completely the problem of accidental singularities in the solution of the Euler–Lagrange equations of motion for a body of arbitrary shape. Thus quaternions are very convenient from the numerical point of view and we found their introduction competitive also in respect of computer time, even though a fourth equation of motion has to be used. On the other hand Euler angles and quantities connected with that parameterization, such as Wigner rotation matrices etc. are invaluable in the formal theoretical description of anisotropic systems. Moreover, probably due to their long periods of neglect, literature on quaternions seems to be rather scarce. We consider it important therefore to make contact between the two formalisms and so we establish in the Appendix the relevant transformations from one parameterization to the other.

The intermolecular potential is easily written in terms of quaternions using the general transformations given in the Appendix. We find

$$U_{ij}=-\epsilon_{ij}P_2(\mathbf{l}^i\cdot\mathbf{l}^j), \tag{4}$$

where

$$l_X{}^i = 2(u_0u_2 + u_1u_3), \tag{5 a}$$

$$l_Y{}^i = -2(u_0u_1 - u_2u_3), \tag{5 b}$$

$$l_Z{}^i = (u_0{}^2 + u_3{}^2 - u_1{}^2 - u_2{}^2), \tag{5 c}$$

are the components of the unit vector **l** defining the symmetry axis of particle i. The torque acting on the ith particle becomes

$$N_a{}^i = 3\epsilon \sum_{\langle ij \rangle} (\mathbf{l}^i \cdot \mathbf{l}^j)\epsilon_{abc} l_b{}^i \, l_c{}^j \; ; \quad a, b, c = X, Y, Z, \tag{6}$$

where the sum is restricted to nearest neighbours and ϵ_{abc} is the Levi-Civita tensor [15]. Summation is implied on repeated tensor indices not appearing on the left hand side. Torque components are calculated in the laboratory frame. They are then transformed to the principal system of the ith molecule employing the rotation matrix, **M**, given in equation (A 19) in terms of quaternions. New angular velocities are then generated by integration of the body frame equations

$$\dot{\omega}_a = N_a / I_{aa} - \epsilon_{abc}\omega_b\omega_c I_{cc}/I_{aa}, \tag{7}$$

where I_{aa} etc. are the principal components of the inertia tensor. Here we consider elongated particles or rather prolate symmetric tops with $I_\parallel / I_\perp = 0{\cdot}2$.

In the usual Euler angles formulation the numerical problem starts at the point when new velocities $\dot{\alpha}$, $\dot{\beta}$, $\dot{\gamma}$, and new angles α, β, γ have to be obtained through a possibly singular transformation. In the quaternion formalism new orientations are instead generated in a straightforward manner by integrating, e.g. for the ith molecule, the equation

$$\begin{pmatrix} \dot{u}_0{}^i \\ \dot{u}_1{}^i \\ \dot{u}_2{}^i \\ \dot{u}_3{}^i \end{pmatrix} = -\frac{1}{2} \begin{pmatrix} u_1 & +u_2 & u_3 & u_0 \\ -u_0 & +u_3 & -u_2 & u_1 \\ -u_3 & +u_0 & u_1 & u_2 \\ u_2 & +u_1 & -u_0 & u_3 \end{pmatrix} \begin{pmatrix} \omega_x{}^i \\ \omega_y{}^i \\ \omega_z{}^i \\ 0 \end{pmatrix}. \tag{8}$$

Equation (8) is obtained in a way similar to that of Evans [14] by inverting the equation

$$\omega_i = -\tfrac{1}{2}\epsilon_{ijk} M_{jl} \dot{M}_{kl} \tag{9}$$

for the components of the angular velocity vector in terms of the rotation matrix **M** components (*cf.* equation (A 19)). The numerical integration of equations (7) and (8) is performed using a fourth order Runge–Kutta–Gill procedure. Although slightly time consuming in comparison with other algorithms this method has some advantages, for example it is self starting and stable as discussed by Berne *et al.* [7 (c)]. Calculations were run on a system composed of 1000 particles, i.e. a $10 \times 10 \times 10$ lattice with periodic boundary conditions.

As usual a molecular dynamics simulation can be divided into three stages : an equilibration, an evolution and production one and finally a third stage in which properties of interest are calculated. In the first part of the calculation the system is started from a given point in phase space and it has to relax to equilibrium. In principle any starting state can be chosen. In practice, since

the system can be followed only for a limited amount of time it is of great importance to consider the equilibration process in some detail. Since we are only interested in equilibrium dynamics the ideal starting state would be itself an equilibrium one. In fact, initial angular velocities do not constitute a problem since they can be sampled from an equilibrium maxwellian distribution. For the orientations we used whenever possible an initial equilibrium orientational configuration taken from a previous Monte Carlo run [5]. On the other hand Monte Carlo configurations may not be always available and we have found starting from a random or a completely aligned configuration unsatisfactory in terms of the time needed to reach equilibrium. We have thus devised a simple alternative procedure to generate an initial configuration not too far from equilibrium. This consists of sampling orientations from a Maier–Saupe type distribution

$$f(\cos\beta) = \exp(\xi \cos^2\beta)/Z, \tag{10}$$

where Z is a normalization constant. The strength parameter ξ is chosen so that $f(\cos\beta)$ yields an approximate value of $\langle P_2 \rangle$ as obtained by interpolating the available Monte Carlo data. The method can obviously be generalized for other potentials and also applied to situations where Monte Carlo data are not available in order to produce approximate starting configurations. The angle β in equation (10) is the angle between the long molecular axis and the director. Thus sampling orientations from equation (10) implicitly defines a director along, say, the laboratory Z axis. Notice that if the starting configuration is obtained from a Monte Carlo run the director will not normally be found along Z. In this case it is useful to transform from the laboratory frame to the director frame by employing the rotation matrix **R** that diagonalizes the ordering tensor for the chosen configuration. We shall come back to this point later when discussing some advantages of the molecular dynamics method.

After choosing an approximately equilibrium initial configuration an equilibration stage followed. This was typically 3000 time steps, with every time step of length $t^* = 0{\cdot}005$. We use throughout dimensionless time t^* and temperature T^* defined by

$$t^* = t(\epsilon/I_\perp)^{1/2}, \tag{11}$$

$$T^* = kT/\epsilon. \tag{12}$$

During this computational stage angular velocities were scaled every 50 time steps so as to reproduce the kinetic energy corresponding to the desired temperature. The equilibration run is stopped when, after scaling, the continuously monitored temperature and order parameter fluctuate about an average value without noticeable drift. This is further checked in the following production stage.

During production the system evolves without any further velocity scaling which would amount to placing it in contact with a thermal reservoir at the desired temperature. Therefore conditions are essentially microcanonical and energy and angular momentum are conserved. This has to be experimentally verified and it represents a test on the goodness of the integration of the equations of motion. By employing a time step of 0·0025 during the production run we obtain energy conservation to better than 10^{-5} per cent over a run of 2500 steps. Similarly we find that the angular momentum J is conserved to better than 10^{-6} in comparison with its initially chosen value of zero.

It is worth noticing that energy conservation (microcanonical conditions) leads for systems with only attractive forces like the present one to some consequences which may seem surprising at first. For example a fluctuation leading to an increase in temperature can also bring about an increase in order. To show that this is the case we consider the total energy E

$$E = K + U, \tag{13}$$

where the kinetic energy K is

$$K = \tfrac{1}{2}\left\langle \sum_{i=1}^{N} \boldsymbol{\omega}^i \mathbf{I}^i \boldsymbol{\omega}^i \right\rangle, \tag{14 a}$$

$$= \tfrac{1}{2} N k n_r T, \tag{14 b}$$

where n_r is the number of degrees of freedom. The potential energy (10) for the present lattice model is

$$U = -\tfrac{1}{2} N \epsilon z \sigma_2, \tag{15}$$

where $z = 6$ is the number of nearest neighbours and σ_2 is the short range order parameter defined [10] as

$$\sigma_2 = \langle P_2(\cos \beta_{ij}) \rangle, \tag{16}$$

with β_{ij} the relative orientation of two nearest neighbour molecules. Considering the differential dE, which is seen to be zero from energy conservation i.e.

$$dE = \frac{\partial E}{\partial T} dT + \frac{\partial E}{\partial \sigma_2} d\sigma_2 = 0, \tag{17}$$

yields

$$\frac{d\sigma_2}{dT} > 0, \tag{18}$$

since $\partial E/\partial T$ is positive and $\partial E/\partial \sigma_2$ is negative for our potential as long as the coupling constant ϵ is greater than zero. What we have said applies to the short range order σ_2 but we expect it to apply also to the normal long range order $\langle P_2 \rangle$ provided $d\sigma_2/d\langle P_2 \rangle > 0$, which could be the case below the transition. Fluctuations in our simulation runs seem to conform to these simple findings. During the production stage orientations and angular velocities were stored on magnetic tape for further analysis every two time steps of 0·0025.

The definition and calculation of the main observables as well as our results are introduced in the next sections.

3. Static properties

The description of the relevant properties in a computer simulation of an anisotropic system as well as some of the techniques for their calculation have been described in detail elsewhere [5]. Single particle information is contained in an infinite set of orientational order parameters. These correspond to coefficients in the expansion of the singlet distribution $P(\alpha, \beta)$ in a Wigner rotation matrix basis set. For a system of uniaxial particles

$$P(\alpha, \beta) = \sum \frac{2L+1}{8\pi^2} \langle D_{m0}^{L*} \rangle D_{m0}^{L}(\alpha \beta 0), \tag{19}$$

where α and β are Euler angles [12]. The molecular dynamics method presents some advantages over the Monte Carlo method for the calculation of static properties. This arises because the time scales for molecular and director reorientation are normally well separated ; in a real system separations are usually larger than 3–4 decades. This means that, since in molecular dynamics we follow the true evolution in time, we can prepare the system as described earlier with a certain director orientation and let it reach orientational equilibrium while preserving the average orientation. If molecular orientational equilibrium has characteristic times much shorter than director relaxation times we can then calculate static (and dynamic) properties considering the director as essentially

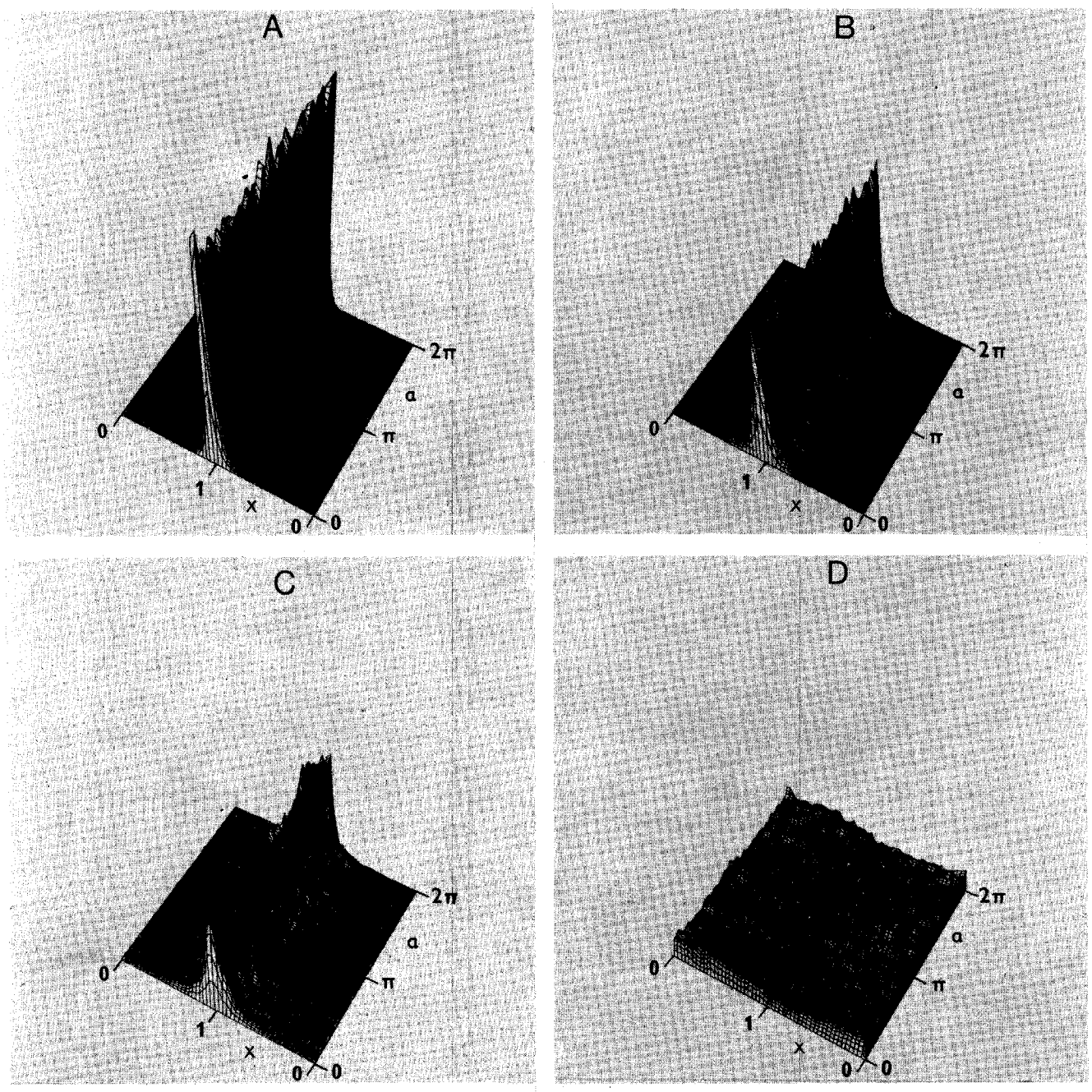

Figure 1. A histogram of the singlet orientational distribution function $P(\alpha, \chi)$, $\chi = |\cos \beta|$ for the model potential in equation (1) as obtained by molecular dynamics simulation. Results shown for $kT/\epsilon = 0{\cdot}50$ (*A*), 0·79 (*B*), 0·88 (*C*) and 1·30 (*D*).

fixed in space. On the contrary in the Monte Carlo method we do not sample equilibrium configurations sequentially in time but rather in a random way. Thus there is in general no guarantee that the director orientation is conserved in the absence of an external constraint. A practical consequence of director conservation is that we can employ molecular dynamics to obtain the full singlet distribution $P(\alpha, \beta)$ as a histogram. This experimental distribution is shown in figure 1 (*a*) to 1 (*d*) for four temperatures ; three of these temperatures are below the orientational phase transition, i.e. $T^* = 0{\cdot}50$, $0{\cdot}79$, $0{\cdot}88$ and one above it, i.e. $T^* = 1{\cdot}30$. It is apparent that $P(\alpha, \beta)$ is essentially independent of the angle α as expected. Above the transition, which is known to take place at about $T^* = 1{\cdot}119$ [3–5], isotropy is restored and all orientations become equally probable ; the histogram appears flat apart from statistical fluctuations. The singlet distribution $P(\alpha, \beta)$ can obviously be employed to calculate order parameters from the definition

$$\langle P_L \rangle = \int_{-1}^{1} d\kappa \, P(\kappa) P_L(\kappa) \Big/ \int_{-1}^{1} d\kappa \, P(\kappa) \, ; \quad \kappa = \cos \beta, \tag{20}$$

where $P(\kappa)$ is obtained by integrating $P(\alpha, \kappa)$ with respect to α. In view of the uniaxiality found we shall from now on consider only $P(\kappa)$. The order parameters of second, fourth and sixth rank obtained by this direct integration method are reported in table 1. The second rank order parameter $\langle P_2 \rangle$ has also been

Table 1. The orientational order parameters $\langle P_2 \rangle$, $\langle P_4 \rangle$, $\langle P_6 \rangle$ at three temperatures T^* as obtained (*a*) by direct integration from the probability distribution $P(\alpha, \kappa)$, $\kappa = \cos \beta$ stored as a 36×360 histogram and (*b*) the order parameter $\langle P_2 \rangle$ obtained by the diagonalization procedure. Production run of 3360 time steps. Also reported (*c*), for comparison, is the value of $\langle P_4 \rangle$ corresponding to $\langle P_2 \rangle$ (*b*) according to the Maier–Saupe theory.

T^*	$\langle P_2 \rangle$ (*b*)	$\langle P_2 \rangle$ (*a*)	$\langle P_4 \rangle$ (*a*)	$\langle P_4 \rangle$ (*c*)	$\langle P_6 \rangle$ (*a*)
0·68	0·833	0·832	0·548	0·55	0·292
0·95	0·626	0·612	0·217	0·254	0·05
1·30	0·09	−0·04	0·003	0·0	0·002

calculated using Vieillard–Baron's method [5]. This consists of calculating, in the course of the production run, the average of the second rank ordering tensor $\mathbf{Q}$

$$\mathbf{Q} = \frac{1}{N} \sum_{i=1}^{N} \mathbf{l}^i \mathbf{l}^i - \tfrac{1}{3}\mathbf{E}, \tag{21}$$

where $\mathbf{E}$ is the identity matrix. The tensor $\mathbf{Q}$ is then diagonalized and the order parameter $\langle P_2 \rangle$ obtained from its largest eigenvalue $\lambda_{\max}$ as [5]

$$\langle P_2 \rangle = \tfrac{3}{2} \lambda_{\max}. \tag{22}$$

Results for $\langle P_2 \rangle$ obtained in this way are also reported in table 1. It is seen that the order parameters calculated in these two ways are in reasonable agreement. The diagonalization procedure does not rely on a knowledge of director orientation and so it is suitable for Monte Carlo calculations as well. It should be

noticed however that the generalization to calculation of higher rank order parameters is not straightforward. Thus one advantage of the molecular dynamics method for anisotropic systems seems the possibility of obtaining higher rank order parameters in a simple way.

4. Dynamics

The description of single particle static orientational quantities can be effected in terms of the singlet orientational distribution $P(\Omega)$, $\Omega=(\alpha\beta\gamma)$. Similarly the description of single particle orientational dynamics can be realized in terms of a joint probability distribution function $P(\Omega_0 0\ ;\ \Omega t)$. This gives the probability that the orientation of a particle is Ω_0 at time zero and Ω at time t. $P(\Omega_0 0\ ;\ \Omega t)$ can be expanded for $t\neq 0$ in a product basis set of Wigner functions :

$$P(\Omega_0 0\ ;\ \Omega t)=\sum P^{LL'}{}_{mn,m'n'}(t)D_{mn}{}^{L}(\Omega_0)D_{m'n'}{}^{L'*}(\Omega), \tag{23}$$

where the expansion coefficients are obtained as

$$P^{LL'}{}_{mn,m'n'}(t)=\frac{(2L+1)(2L'+1)}{64\pi^4}\langle D_{mn}{}^{L*}(\Omega_0)D_{m'n'}{}^{L'}(\Omega)\rangle, \tag{24}$$

by using the orthogonality of the Wigner functions. Equation (23) can be simplified using the methods described in [10] to take advantage of the symmetry of the mesophase and of the constituent particles. For a uniaxial mesophase a rotation about the Z axis, chosen to be along the director should leave $P(\Omega_0 0\ ;\ \Omega t)$ invariant. However, under such a rotation equation (23) becomes

$$R_z(\alpha)P(\Omega_0 0\ ;\ \Omega t)=\sum P^{LL'}{}_{mn,m'n'}(t)\exp\left[-i\alpha(m-m')\right] \times D_{mn}{}^{L}(\Omega_0)D_{m'n'}{}^{L'*}(\Omega). \tag{25}$$

The required projection on the totally symmetric representation amounts to an integration over α. The requisite of invariance therefore yields $\delta_{m,m'}$ in equation (25). Similarly if the constituent particles are also cylindrically symmetric a rotation about the molecular symmetry axis should leave the distribution invariant and $\delta_{n,n'}$ is obtained. For such a system

$$P(\Omega_0 0\ ;\ \Omega t)=\sum P^{LL'}{}_{mn,m'n'}(t)D_{mn}{}^{L}(\Omega_0)D_{m'n'}{}^{L'*}(\Omega)\delta_{m,m'}\,\delta_{n,n'} \tag{26}$$

and the expansion coefficients are, apart from a numerical factor, the Wigner rotation matrix correlation functions

$$\phi_{mn}{}^{LL'}(t)\equiv\langle D_{mn}{}^{L*}(\Omega_0)D_{mn}{}^{L'}(\Omega)\rangle. \tag{27}$$

These orientational correlation functions give therefore progressively more information about the joint orientational distribution of the system. Since it is fairly impractical to build and store a multi dimensional histogram of $P(\Omega_0 0\ ;\ \Omega t)$ the knowledge of the $\phi_{mn}{}^{LL'}(t)$ provides us with a systematic approach to the orientational dynamics. In fact only the orientational correlations of the lowest rank $L=1$, $L=2$ or their Fourier transforms will be required to interpret most experimental data. A notable exception is represented by neutron scattering, where in principle correlation functions of every rank can contribute. In figures 2–6 our results for the correlation functions of the Wigner rotation matrices are shown for three temperatures : two in the ordered phase ($T^*=0{\cdot}68$, $0{\cdot}95$)

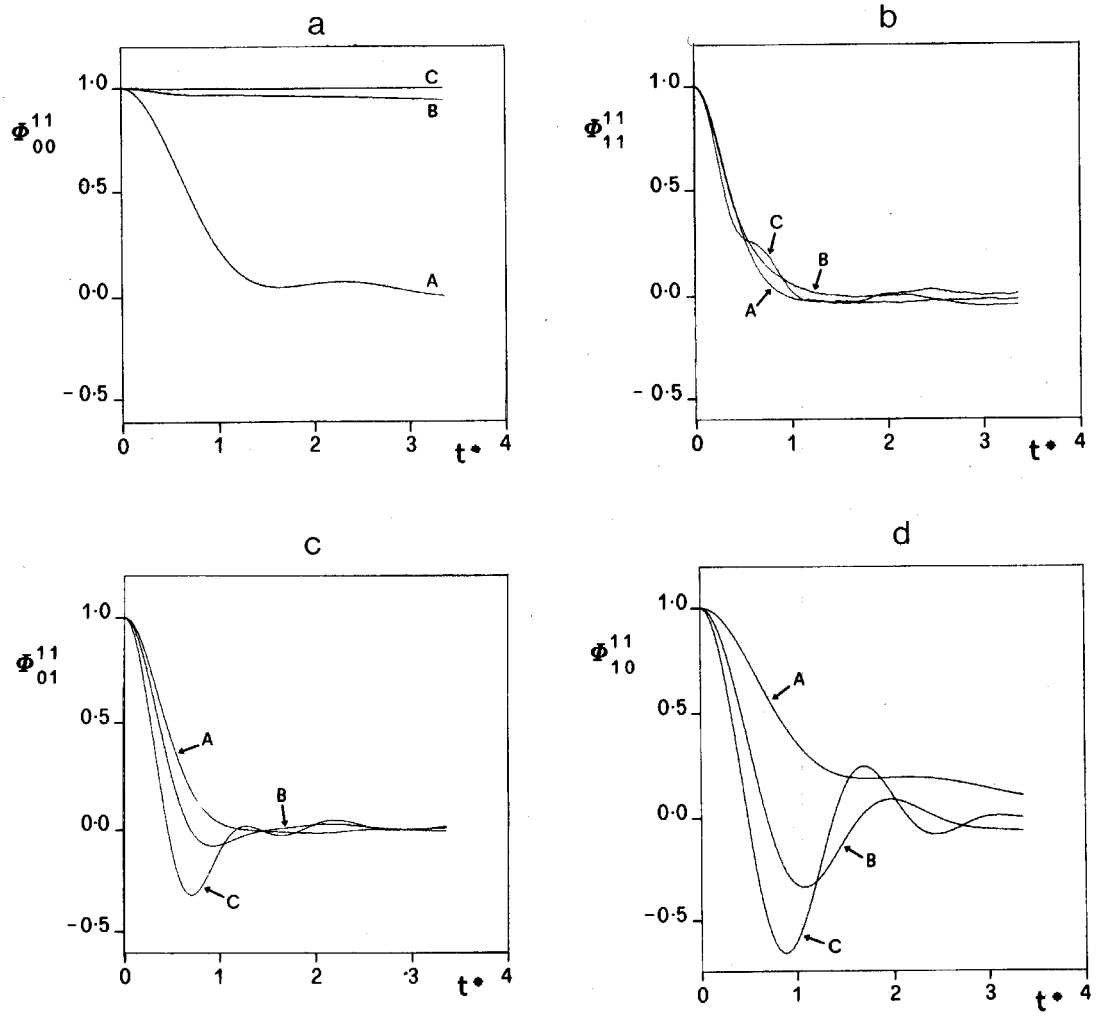

Figure 2. The first rank orientational correlation functions

$$\Phi_{mn}^{11}(t) = \mathrm{Re}\,\langle D_{mn}^{1*}(0) D_{mn}^{1}(t)\rangle / \langle D_{mn}^{1*}(0) D_{mn}^{1}(0)\rangle$$

versus time in reduced units for three temperatures T^* equal to (A) 1·30, (B) 0·95, (C) 0·68 ; (a) $\Phi_{00}^{11}(t)$, (b) $\Phi_{11}^{11}(t)$, (c) $\Phi_{01}^{11}(t)$, (d) $\Phi_{10}^{11}(t)$ are shown.

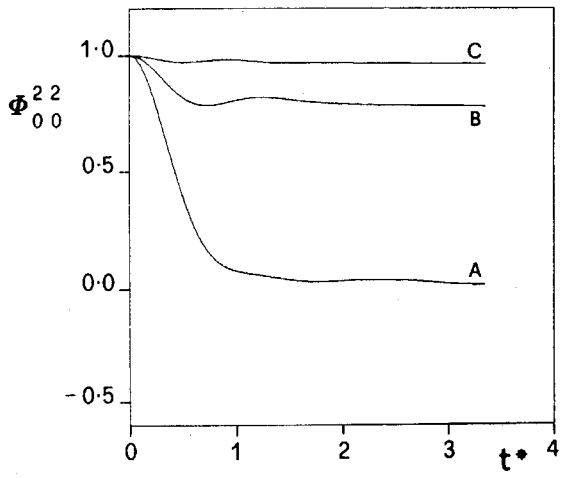

Figure 3. The second rank orientational correlation function

$$\Phi_{00}^{22}(t) = \langle D_{00}^{2*}(0) D_{00}^{2}(t)\rangle / \langle D_{00}^{2*}(0) D_{00}^{2}(0)\rangle$$

versus reduced time t^* for temperatures T^* equal to (A) 1·30, (B) 0·95, (C) 0·68.

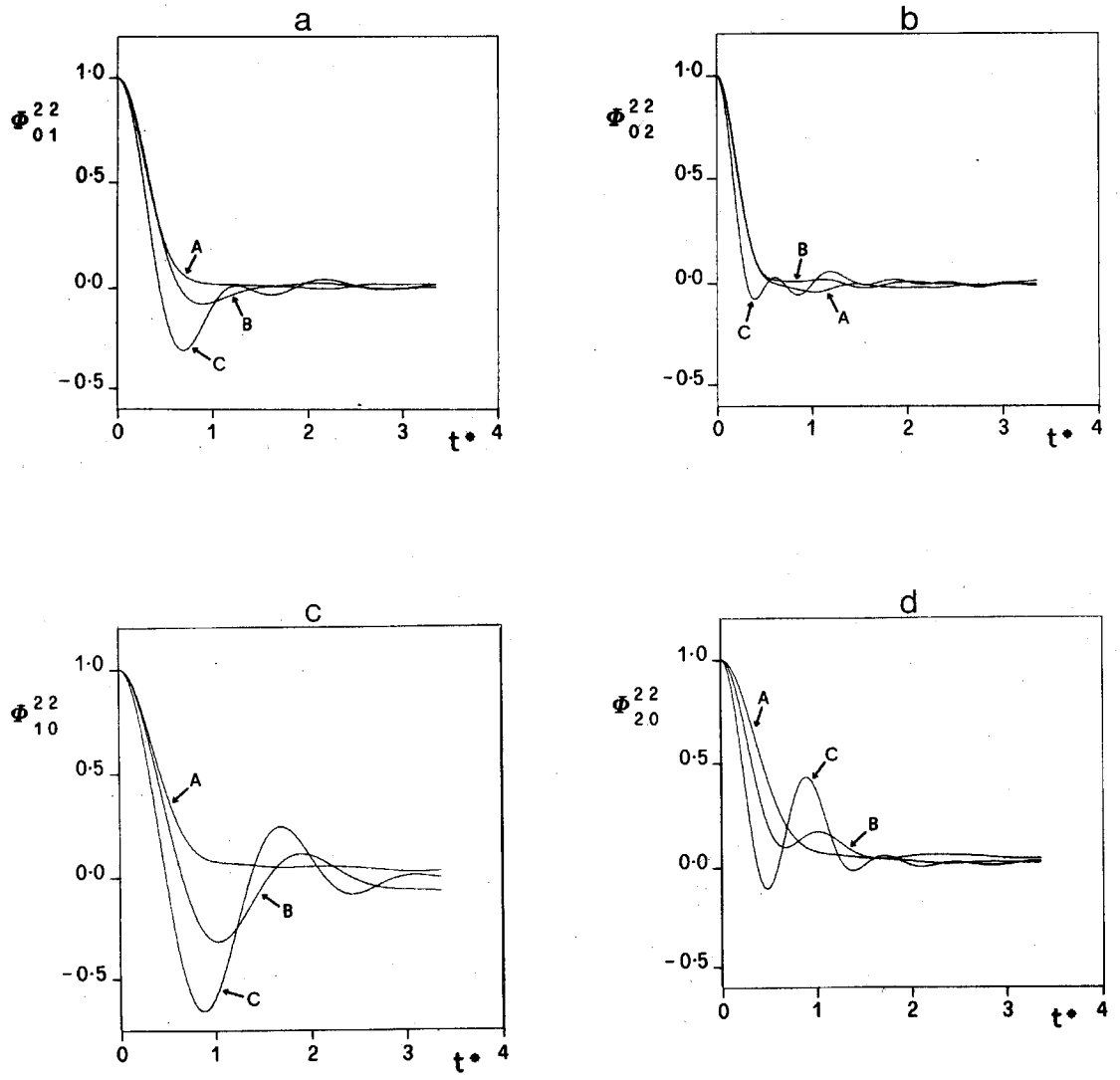

Figure 4. Second rank orientational correlation functions

$$\Phi_{mn}{}^{22}(t) = \mathrm{Re}\,\langle D_{mn}{}^{2*}(0) D_{mn}{}^{2}(t)\rangle / \langle D_{mn}{}^{2*}(0) D_{mn}{}^{2}(t)\rangle$$

versus reduced time t^* for temperatures T^* equal to (A) 1·30, (B) 0·95, (C) 0·68. Shown here are (a) $\Phi_{01}{}^{22}(t)$, (b) $\Phi_{02}{}^{22}(t)$, (c) $\Phi_{10}{}^{22}(t)$, (d) $\Phi_{20}{}^{22}(t)$.

and one in the isotropic phase ($T^* = 1{\cdot}30$). In these figures we give the correlations $\Phi_{mn}{}^{LL'}(t)$ normalized to a value of unity at time $t^* = 0$, i.e.

$$\Phi_{mn}{}^{LL'}(t) \equiv \langle D_{mn}{}^{L*}(\Omega_0) D_{mn}{}^{L'}(\Omega)\rangle / \langle D_{mn}{}^{L*}(\Omega_0) D_{mn}{}^{L'}(\Omega_0)\rangle, \qquad (28\,a)$$

$$\equiv \phi_{mn}{}^{LL'}(t) / \phi_{mn}{}^{LL'}(0). \qquad (28\,b)$$

The initial values of the correlation function $\phi_{mn}{}^{LL'}(t)$ can be calculated using the Clebsch–Gordan series. For a uniaxial probe and anisotropic phase we find

$$\phi_{mn}{}^{LL'}(0) = (-)^{m-n} \sum_J C(LL'J\,;\; m-m) C(LL'J\,;\; n-n) \langle P_J \rangle, \qquad (29)$$

where $C(abc\,;\; de)$ is a Clebsch–Gordan coefficient [12]. In practice we are interested in functions of rank L, $L' = 1$, 2 and the explicit expressions for these

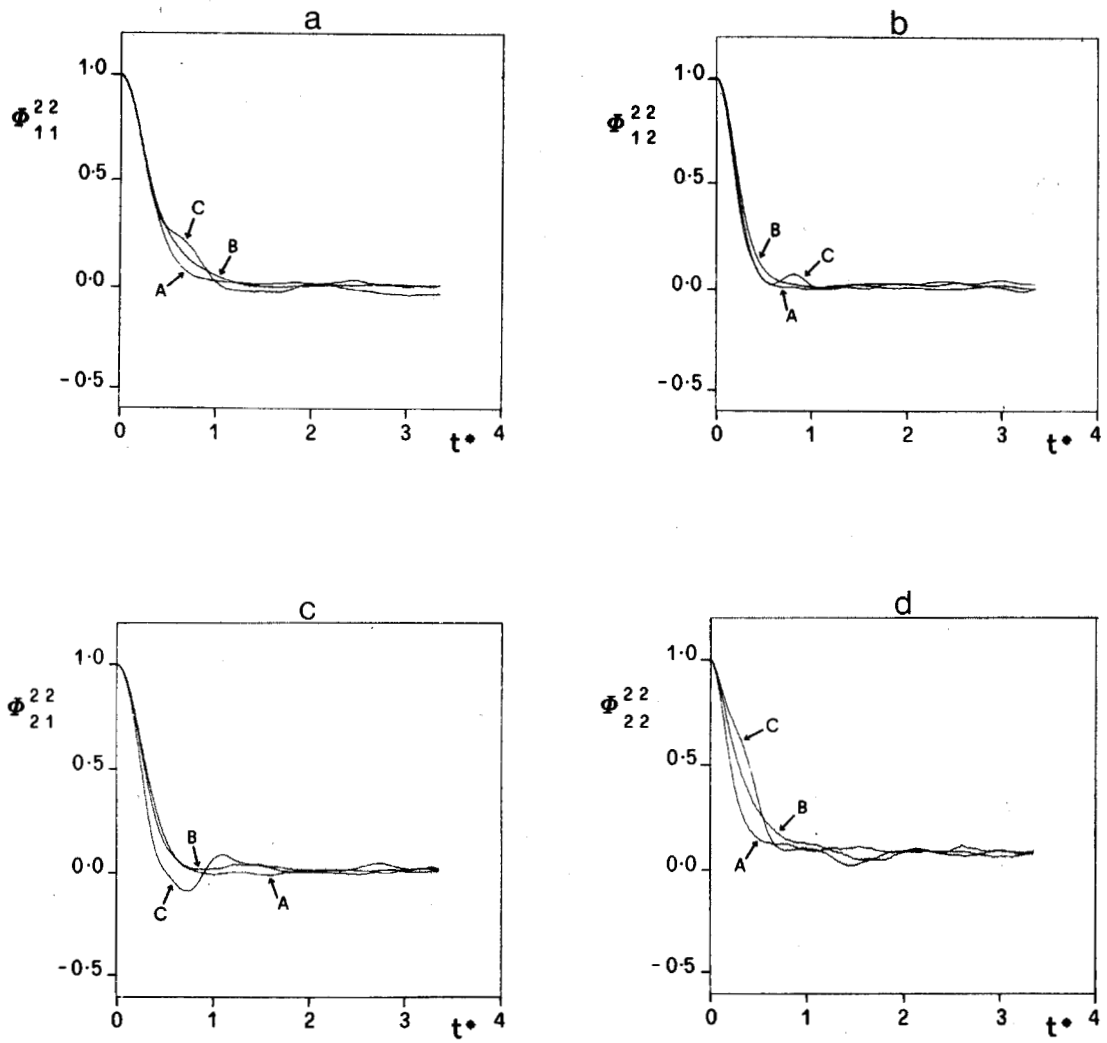

Figure 5. The orientational correlation functions

$$\Phi_{mn}{}^{22}(t) = \mathrm{Re}\,\langle D_{mn}{}^{2*}(0) D_{mn}{}^{2}(t)\rangle / \langle D_{mn}{}^{2*}(0) D_{mn}{}^{2}(0)\rangle$$

(*a*) $\Phi_{11}{}^{22}(t)$, (*b*) $\Phi_{12}{}^{22}(t)$, (*c*) $\Phi_{21}{}^{22}(t)$, (*d*) $\Phi_{22}{}^{22}(t)$ shown as a function of time in reduced units for T^* equal to (*A*) 1·30, (*B*) 0·95, (*C*) 0·68.

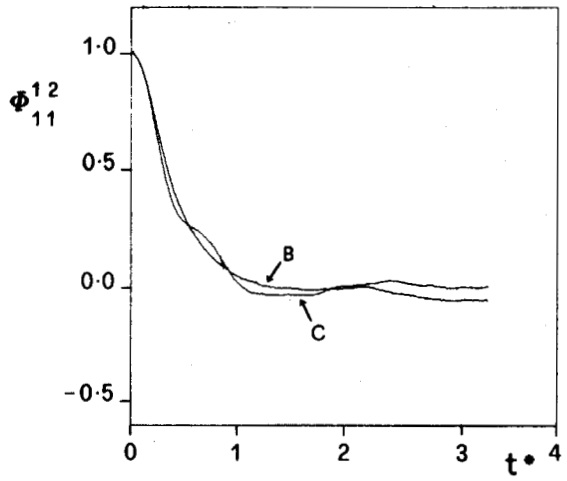

Figure 6. The mixed rank orientational correlation function

$$\Phi_{11}{}^{12}(t) = \mathrm{Re}\,\langle D_{11}{}^{1*}(0) D_{11}{}^{2}(t)\rangle / \langle D_{11}{}^{1*}(0) D_{11}{}^{2}(0)\rangle$$

shown for two temperatures in the ordered phase (*B*) 0·95 and (*C*) 0·68.

Table 2. Explicit expressions for the initial values of the Wigner rotation matrix correlation functions $\phi_{mn}^{LL'}(0) = \langle D_{mn}^{L*} D_{mn}^{L'} \rangle$ with L, $L' = 1, 2$ for cylindrically symmetric molecules and a uniaxial mesophase.

L	L'	m	n	$\phi_{mn}^{LL'}(0)$
1	1	0	0	$\frac{1}{3}+2\langle P_2\rangle/3$
1	1	0	±1	$\frac{1}{3}-\langle P_2\rangle/3$
1	1	±1	0	$\frac{1}{3}-\langle P_2\rangle/3$
1	1	±1	±1	$\frac{1}{3}+\langle P_2\rangle/6$
1	2	0	0	0
1	2	0	±1	0
1	2	±1	0	0
1	2	±1	±1	$\langle P_2\rangle/2$
2	2	0	0	$\frac{1}{5}+2\langle P_2\rangle/7+18\langle P_4\rangle/35$
2	2	0	±1	$\frac{1}{5}+\langle P_2\rangle/7-12\langle P_4\rangle/35$
2	2	0	±2	$\frac{1}{5}-2\langle P_2\rangle/7+3\langle P_4\rangle/35$
2	2	±1	0	$\frac{1}{5}+\langle P_2\rangle/7-12\langle P_4\rangle/35$
2	2	±1	±1	$\frac{1}{5}+\langle P_2\rangle/14+8\langle P_4\rangle/35$
2	2	±1	±2	$\frac{1}{5}-\langle P_2\rangle/7-4\langle P_4\rangle/70$
2	2	±2	0	$\frac{1}{5}-2\langle P_2\rangle/7+3\langle P_4\rangle/35$
2	2	±2	±1	$\frac{1}{5}-\langle P_2\rangle/7-2\langle P_4\rangle/35$
2	2	±2	±2	$\frac{1}{5}+2\langle P_2\rangle/7+\langle P_4\rangle/70$

$\phi_{mn}^{LL'}$ are given in table 2. As we can see the initial values depend on the order parameter $\langle P_2\rangle$ for the first rank correlation functions. However the second rank correlations starting values $\phi_{mn}^{22}(0)$ depend on the fourth rank order parameter $\langle P_4\rangle$ as well as on $\langle P_2\rangle$. In some experiments, e.g. in fluorescence depolarization studies, this dependence can be of value to extract the order parameter $\langle P_4\rangle$ [16]. The same could be done for the simulation results. Alternatively the relations in table 2 can be used to provide a check on the order parameters $\langle P_2\rangle$ and $\langle P_4\rangle$ previously determined. This is shown in table 3, where we give values for $\phi_{mn}^{LL'}(0)$ obtained from the correlation function calculation and compare them with the values in brackets obtained through the expressions in table 2 and the order parameters in table 1. The agreement is seen to be satisfactory.

The Wigner matrix correlation functions needed to describe the orientational dynamics of anisotropic systems are, to a given rank, many more than those required for isotropic fluids. More importantly the correlations at a given time are not just a function of the angle between the two orientations at time zero and time t, but depend on the starting orientation Ω_0 as well. To discuss the differences and similarities with isotropic systems, we obtain first the equivalent of equation (26) for such systems by imposing the additional requirement of rotational invariance. Under a rotation $R(\Omega')$ of the laboratory frame equation (23) becomes

$$P(\Omega_0 0\,;\ \Omega t) = \sum P^{LL'}{}_{mn,m'n'}(t) D_{qn}^{L}(\Omega_0) D_{q'n'}^{L'*}(\Omega) \times D_{qm}^{L*}(\Omega') D_{q'm'}^{L'}(\Omega'). \quad (30)$$

Table 3. Initial values of the Wigner correlation functions $\phi_{mn}{}^{LL'}$ at three temperatures as obtained directly from the correlation function compared with the value obtained from the order parameter $\langle P_2 \rangle$ and $\langle P_4 \rangle$ extracted from the histograms and the expressions in table 2 (in brackets).

$\phi_{mn}{}^{LL'}$	$T^*=0{\cdot}68$	$T^*=0{\cdot}95$	$T^*=1{\cdot}30$
$\phi_{00}{}^{11}$	0·889 (0·888)	0·742 (0·741)	0·305 (0·307)
$\phi_{0\pm1}{}^{11}=\phi_{\pm10}{}^{11}$	0·056 (0·056)	0·129 (0·129)	0·347 (0·347)
$\phi_{\pm1,\pm1}{}^{11}$	0·471 (0·472)	0·435 (0·435)	0·336 (0·327)
$\phi_{00}{}^{12}$	−0·001 (0·000)	−0·003 (0·000)	0·007 (0·000)
$\phi_{\pm10}{}^{12}=\phi_{0\pm1}{}^{12}$	−0·0004 (0·000)	0·001 (0·000)	0·007 (0·000)
$\phi_{\pm1\pm1}{}^{12}$	0·416 (0·416)	0·305 (0·306)	−0·015 (−0·020)
$\phi_{00}{}^{22}$	0·720 (0·719)	0·487 (0·486)	0·190 (0·190)
$\phi_{0\pm1}{}^{22}=\phi_{\pm10}{}^{22}$	0·131 (0·131)	0·213 (0·213)	0·193 (0·193)
$\phi_{0\pm2}{}^{22}=\phi_{\pm20}{}^{22}$	0·009 (0·009)	0·044 (0·044)	0·212 (0·212)
$\phi_{\pm1\pm1}{}^{22}$	0·385 (0·385)	0·291 (0·293)	0·199 (0·198)
$\phi_{\pm1\pm2}{}^{22}=\phi_{\pm2\pm1}{}^{22}$	0·049 (0·050)	0·101 (0·100)	0·209 (0·205)
$\phi_{\pm2\pm2}{}^{22}$	0·445 (0·445)	0·377 (0·378)	0·195 (0·189)

Projection onto the invariant representation is obtained by integrating over $d\Omega'/8\pi^2$, which gives

$$P(\Omega_0 0\,;\ \Omega t)=\sum P^{LL'}{}_{mn,m'n'}(2L+1)^{-1}\,\delta_{LL'}\delta_{mm'}\delta_{qq'}D_{qn}{}^{L}(\Omega_0)D_{q'n'}{}^{L'*}(\Omega), \quad (31\,a)$$

$$=\sum\left\{\sum_m P^{LL}{}_{mn,mn'}(2L+1)^{-1}\right\}D_{qn}{}^{L}(\Omega_0)D_{qn'}{}^{L*}(\Omega). \quad (31\,b)$$

The sum over q can be performed using the closure property of the Wigner functions to give

$$P(\Omega_0 0\,;\ \Omega t)=\sum P_{nn'}{}^{L}(t)D_{nn'}{}^{L*}(\Omega_{t0}), \quad (32)$$

where Ω_{t0} is the angle between orientation at time zero and time t

$$P_{nn'}{}^{L}(t)=(2L+1)\langle D_{nn'}{}^{L}(t)\rangle/64\pi^4, \quad (33)$$

while for a symmetric top $\delta_{nn'}$ appears in equation (31). We see therefore that there are two main consequences of a phase being spherically symmetric. One is that only relative orientations Ω_{t0} matter ; for linear or symmetric top molecules the relevant orientational correlations are just $\langle D_{00}{}^{1}(\Omega_{t0})\rangle$, $\langle D_{00}{}^{2}(\Omega_{t0})\rangle$ etc. or in a perhaps more familiar notation $\langle P_1(\mathbf{l}(0)\cdot\mathbf{l}(t))\rangle$, etc. [7]. The second is that mixed rank correlations are forbidden in the isotropic phase. The same is not necessarily true in the ordered phase. In figure 6 we show the mixed rank correlation function $\Phi_{11}{}^{12}(t)$ as calculated for the present simulation. The order parameters themselves could be considered as mixed rank correlations between Wigner rotation matrices of rank zero and of a certain rank. Thus for rank L

$$\langle D_{mn}{}^{L}\rangle=\langle D_{00}{}^{0*}(\Omega_0)D_{mn}{}^{L}(\Omega)\rangle,$$
$$=\phi_{00}{}^{0L}\,\delta_{m0}\delta_{n0}, \quad (34)$$

where as usual we have assumed cylindrically symmetric particles and a uniaxial mesophase. Obviously $\langle D_{mn}{}^{L}\rangle$ is time independent since $D_{00}{}^{0}(\Omega_0)$ is just a constant.

We do not wish to enter at this stage into the problem of establishing what sort of reorientational model [17–19] describes best the set of orientational correlations in figures 2–6. However, it is worth pointing out that the present correlation functions, obtained for a simple anisotropic potential should constitute an interesting test case for theories of reorientation. On the time scale of our experiment the two most popular models of reorientation, i.e. the strong collision and the diffusional both seem inadequate. They are in fact unable to predict, e.g. the vanishing of the first order time derivative of the correlation functions at time zero and the oscillatory behaviour observed.

To elucidate some qualitative aspects of the reorientation problem as well as an aid in verifying the expectations from current models of motion or possibly in suggesting new ones [20] a motion picture of the dynamical evolution of the system has been made [21]. The graphics package developed [21 (a)] allows us to show for example a set of spherocylinders whose trajectory has been

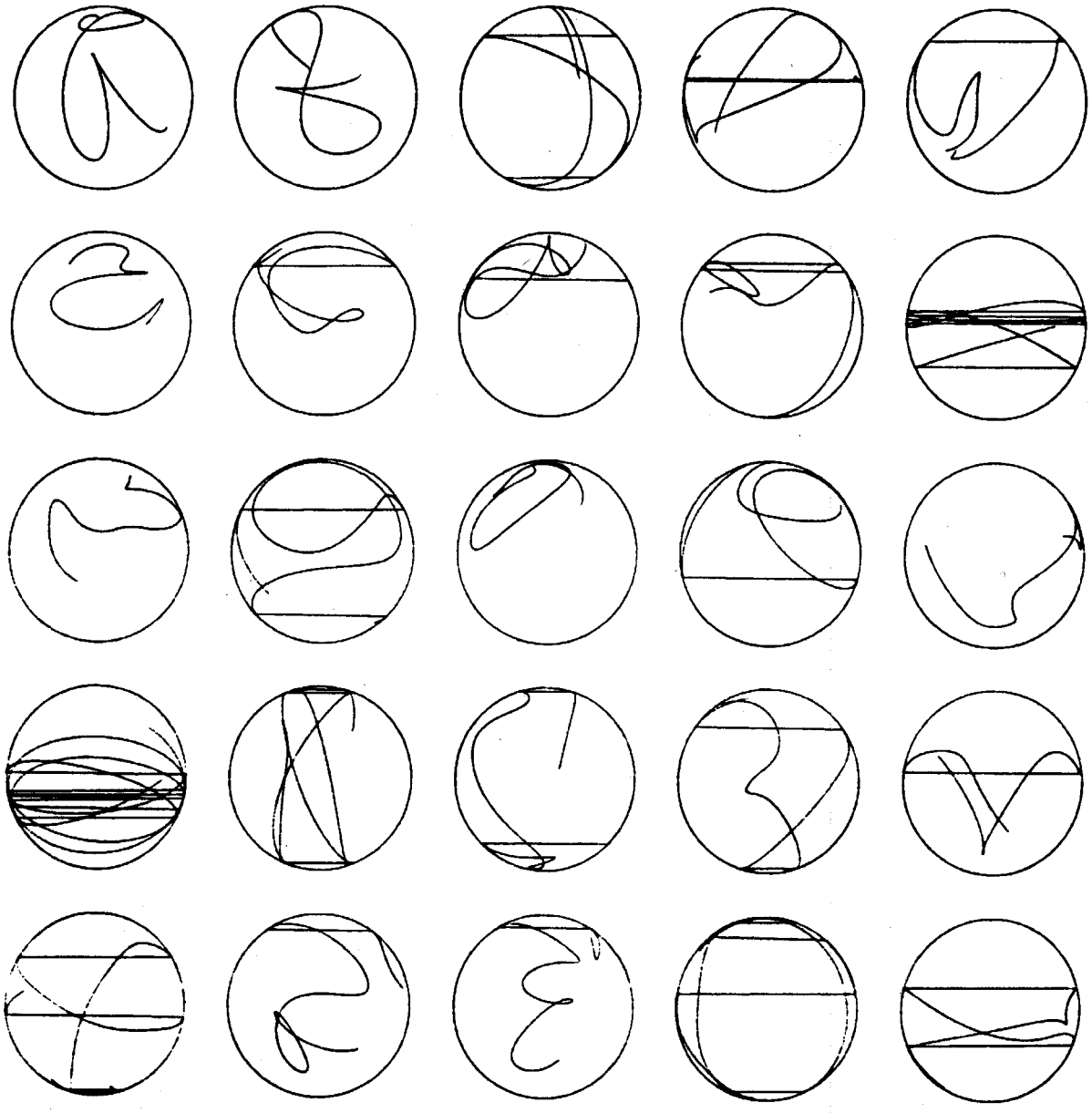

Figure 7 (*a*).

obtained from the molecular dynamics simulation. More simply but perhaps less effectively, we can visualize the evolution of one particle by following the trajectory of the point defining the orientation on the tangent sphere. By projecting this trajectory onto the laboratory ZX plane we have in essence a record of the motion of the long axis of the particle. We have done this for several temperatures and for 500 particles. A subset of 25 of these trajectories is shown in figures 7 (*a*)–7 (*c*) for the same three temperatures : $T^*=0{\cdot}68$, $T^*=0{\cdot}95$ and $T^*=1{\cdot}30$ at which results for the orientational correlation functions were previously calculated. As is apparent from these figures we find that in the ordered phase (at the temperatures studied) reorientation of the long axis is confined essentially to the pole of the sphere where the particle started to be observed. That is, during the observation time, end to end reorientation of the long axis is fairly unlikely, for our system.

Motion on a cone about the director direction, represented as horizontal lines in our ZX view are instead fairly common. While very little statistics can be

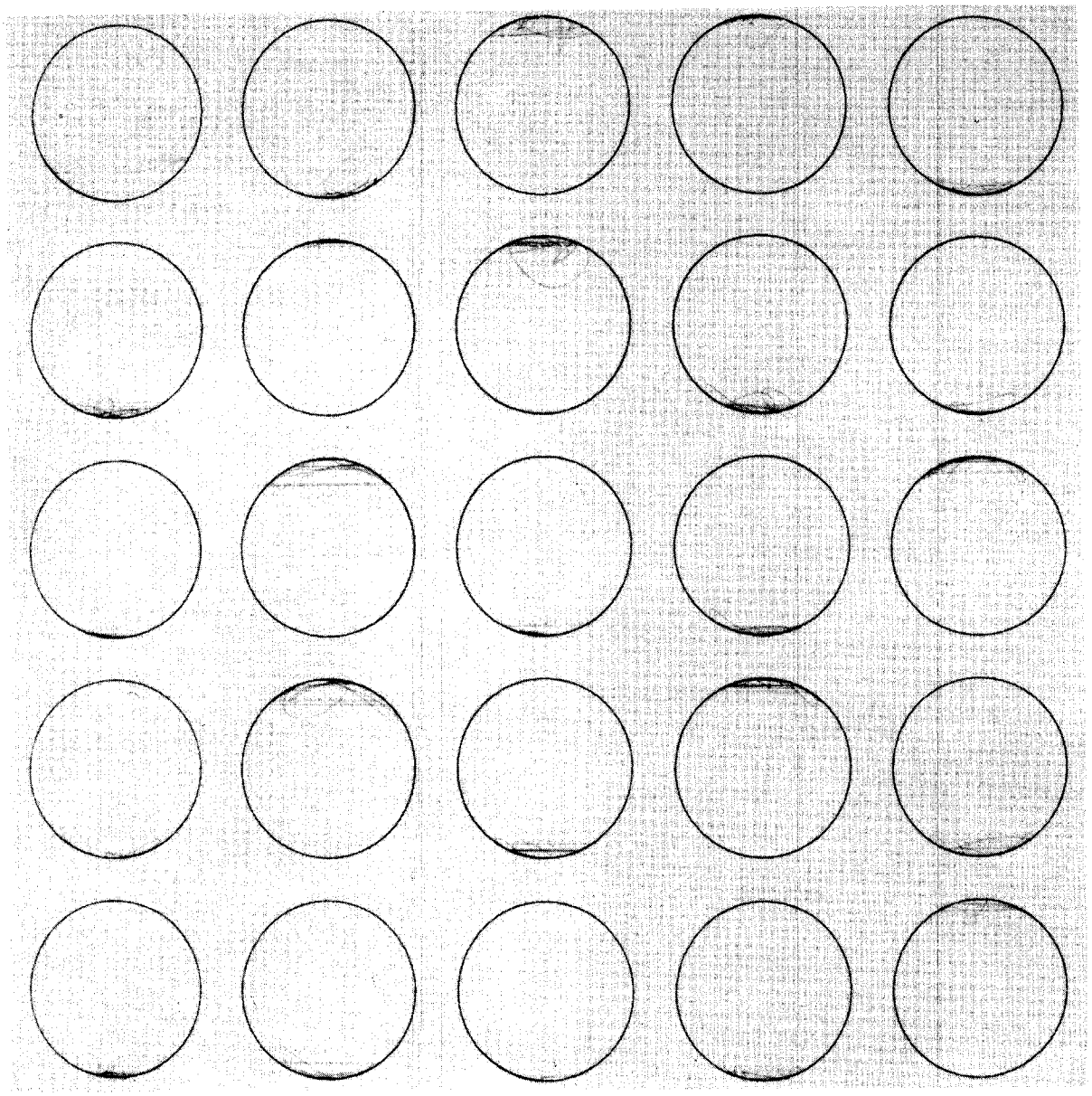

Figure 7 (*b*).

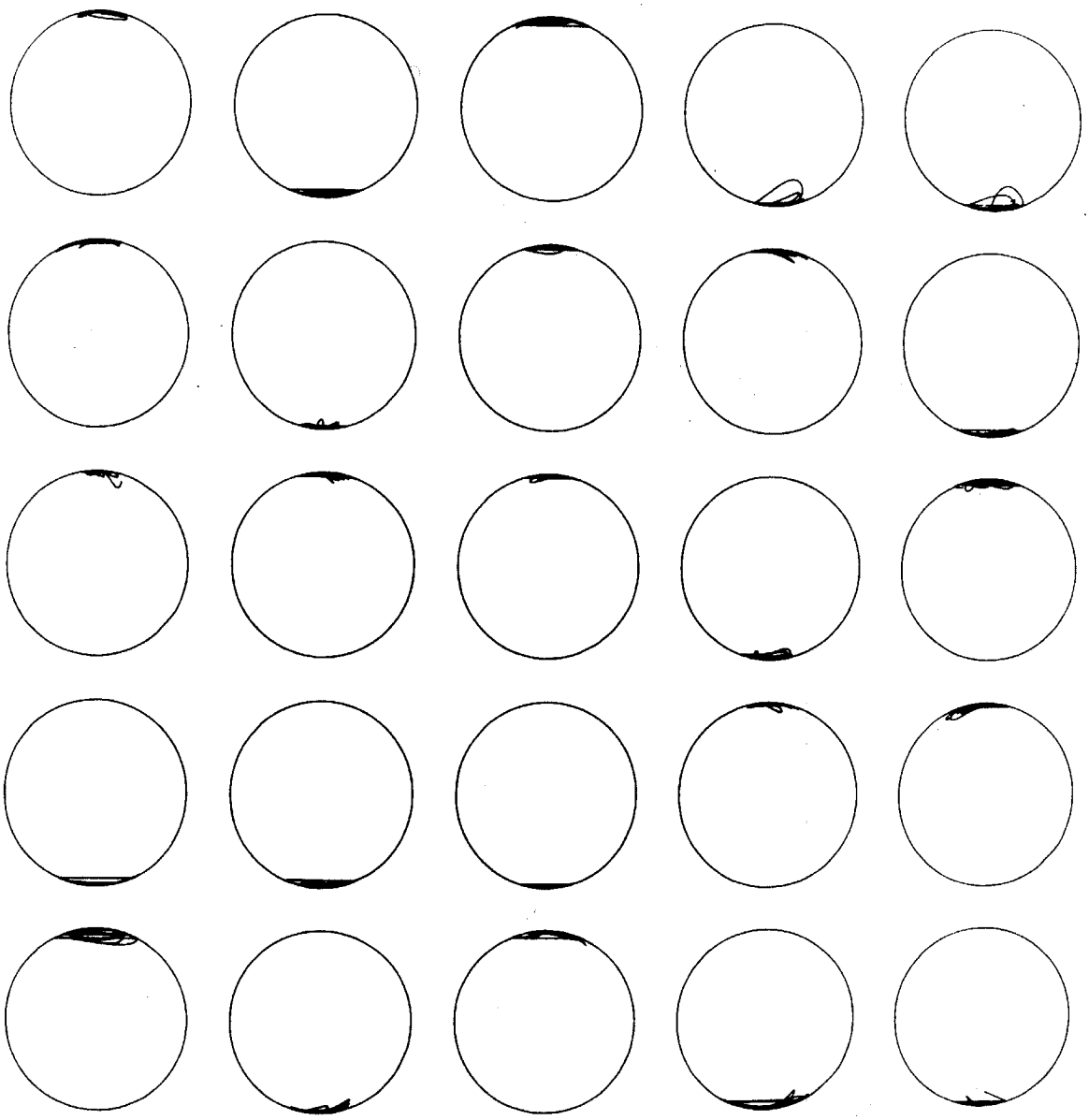

Figure 7 (*c*).

Figure 7. Trajectories of the point representing the orientation of a particle's long axis on the tangent sphere. The director is along Z (vertical) and the ZX view is shown. Results are given for 25 particles out of 1000 and for temperatures T^* of (*a*) 1·30, (*b*) 0·95, (*c*) 0·68. The last two temperatures are in the ordered phase, the first in the isotropic phase.

extracted from such a limited number of particles as shown in figure 7 we may remark that these constitute a typical sample of what we observe for our 500 plotted trajectories. It is of interest to note that the visualization method proposed in figures 7 (*a*)–7 (*c*) affords a simple way of deciding if the whole sample is a monodomain or if instead local structure is present, with the director fluctuating from one point of the sample to the other. In other situations, with external constraints present, it can allow a check of their effectiveness in influencing the director orientation. In our simulations we have found a monodomain structure in the ordered phase. In the isotropic phase no director is present ; from a dynamic point of view the motion is quite free and most of the particles explore the whole of the tangent sphere during the observation time. This is

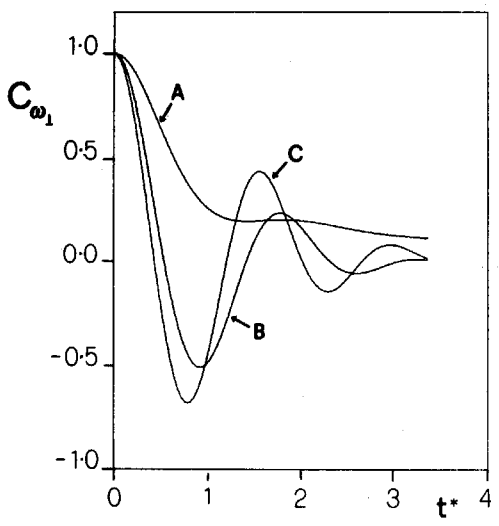

Figure 8. Correlation function $C_{\omega_\perp}(t) = \langle \boldsymbol{\omega}_\perp(0) \cdot \boldsymbol{\omega}_\perp(t) \rangle / \langle \boldsymbol{\omega}_\perp(0) \cdot \boldsymbol{\omega}_\perp(0) \rangle$ of the angular velocity component perpendicular to the molecular symmetry axis. Curves correspond to reduced temperatures (*A*) 1·30, (*B*) 0·95, (*C*) 0·68.

after all quite reasonable since constraints upon the motion come only from the anisotropic potential in equation (1). Thus the motion seems to be fairly inertial as long as the strength of the anisotropic potential is not such as to produce a strong hindrance to rotation [18]. To investigate this we can examine the correlation function $C_{\omega_\perp}(t)$ of the component of the angular velocity perpendicular to the molecular symmetry axis, shown in figure 8. In the isotropic phase the angular velocity correlation $C_{\omega_\perp}(t)$ decays on a time scale similar to that of the various orientational correlations $\Phi_{mn}^{LL'}(t)$. However, in the ordered phase the orientational correlation function $\Phi_{00}^{11}(t)$, which depends only on the long axis reorientation, decays on a time scale very much longer than that of $C_{\omega_\perp}(t)$. The behaviour of the second Legendre polynomial correlation function $\Phi_{00}^{22}(t)$, although apparently similar to that of $\Phi_{00}^{11}(t)$ is in actual fact qualitatively different since the infinite time limit of $\phi_{00}^{22}(t)$ is not zero but the square of the second rank order parameter. The other correlation functions $\Phi_{mn}^{LL}(t)$ do not have very different time scales in the isotropic and nematic phase, which is quite reasonable since they depend not only on the Euler angle β describing long axis reorientation but also on the other Euler angles which vary quite freely for our potential.

Calculations were performed on the CDC7600 at CINECA (Bologna). We are grateful to Ing. E. Corda and Dr. M. E. Ronchi for their collaboration. We wish to thank Dr. P. Pasini for his help with various aspects of the computation. C.Z. acknowledges support from C.N.R. (Italy) and wishes to thank Dr. F. Jorgensen for reading the Appendix and Professor G. R. Luckhurst for a critical discussion of the whole manuscript during a visit made possible by a NATO research grant.

Appendix

A quaternion q is a four component quantity, [14, 22]

$$q = q_0 + q_1 e_1 + q_2 e_2 + q_3 e_3, \qquad \text{(A 1)}$$

where q_i, $i=0, 1, 2, 3$ are real numbers and the basis components e_1, e_2, e_3 obey the combination rule

$$e_i e_j = -\delta_{ij} + \epsilon_{ijk} e_k. \tag{A 2}$$

Since we are interested in making contact with the Euler type description of rotations it is useful to understand that a representation of quaternions can be realized in terms of the Pauli spin matrices σ_1, σ_2, σ_3. Thus if we define the basis $\{e\}$ as

$$e_1 = -i\sigma_1, \quad e_2 = -i\sigma_2, \quad e_3 = -i\sigma_3, \tag{A 3}$$

it is seen that the multiplication law (A 2) is obtained. One of the reasons for our particular interest in quaternions is that they constitute, according to the Frobenius theorem [15], the only algebra, together with real numbers and complex numbers, where every non-null element has an inverse ; this is just

$$q^{-1} = q^*/qq^*. \tag{A 4}$$

It is easily verified using equations (A 1–A 2) or directly from the Pauli matrices that the product of two quaternions

$$q = a + \mathbf{b} \cdot \mathbf{e} \quad \text{and} \quad q' = a' + \mathbf{b}' \cdot \mathbf{e} \tag{A 5}$$

can be written as

$$qq' = (aa' - \mathbf{b} \cdot \mathbf{b}') + [a\mathbf{b}' + \mathbf{a}'\mathbf{b} + (\mathbf{b} \wedge \mathbf{b}')] \cdot \mathbf{e},$$

where a vector notation has been used for compactness.

We now wish to show the connection between rotation operators and quaternions. We start by writing the operator for a right handed rotation of an angle ϑ about an axis $\mathbf{n}$ as [12]

$$R_{\mathbf{n}}(\vartheta) = \exp(-i\vartheta \mathbf{n} \cdot \mathbf{J}), \tag{A 6}$$

where is $\mathbf{J}$ the angular momentum operator. By choosing a spinor representation, $\mathbf{J} = \boldsymbol{\sigma}/2$ and using the isomorphism (A 3), the rotation operator can be rewritten in terms of the quaternion basis $\{\mathbf{e}\}$ as

$$R_{\mathbf{n}}(\vartheta) = \exp\left(\frac{\vartheta}{2} \mathbf{n} \cdot \mathbf{e}\right). \tag{A 7}$$

This shows at once that rotations can be described in terms of quaternions. Using equation (A 5) and the power series for sin and cos it is easy to show that the generalized Euler formula

$$\exp(\lambda \mathbf{n} \cdot \mathbf{e}) = \cos\lambda + (\mathbf{n} \cdot \mathbf{e}) \sin\lambda \tag{A 8}$$

holds. Thus we can also write

$$R_{\mathbf{n}}(\vartheta) = \cos\frac{\vartheta}{2} + (\mathbf{n} \cdot \mathbf{e}) \sin\frac{\vartheta}{2}. \tag{A 9}$$

Clearly this is still a quaternion, u, say, thus

$$R_{\mathbf{n}}(\vartheta) = u_0 + \mathbf{n} \cdot \mathbf{e}, \tag{A 10}$$

where $u_0 = \cos(\vartheta/2)$, $u_1 = n_X \sin(\vartheta/2)$, $u_2 = n_Y \sin(\vartheta/2)$, $u_3 = n_Z \sin(\vartheta/2)$. This shows that quaternions lend themselves naturally to describe a rotation in terms of half angles of rotation and the components of the rotation axis.

We now wish to obtain expressions for ϑ and $\mathbf{n}$ in terms of Rose's definition of Euler angles. This can be done in a number of ways. We choose to start from the rotation operator in terms of laboratory fixed angular momentum operators. We then use again the $\mathbf{J}=\boldsymbol{\sigma}/2$ representation ; thus

$$R(\alpha\beta\gamma)=\exp\left(-i\frac{\alpha}{2}\sigma_Z\right)\exp\left(-i\frac{\beta}{2}\sigma_Y\right)\exp\left(-i\frac{\gamma}{2}\sigma_Z\right), \tag{A 11}$$

$$=\exp\left(\frac{\alpha}{2}e_Z\right)\exp\left(\frac{\beta}{2}e_Y\right)\exp\left(\frac{\gamma}{2}e_Z\right), \tag{A 12}$$

in terms of the quaternion basis. Using repeatedly the generalized Euler formula we find

$$R(\alpha\beta\gamma)=u_0+\mathbf{u}\cdot\mathbf{e}, \tag{A 13}$$

with

$$u_0=\cos\frac{\beta}{2}\cos\frac{\alpha+\gamma}{2}, \tag{A 14 a}$$

$$u_1=-\sin\frac{\beta}{2}\sin\frac{\alpha-\gamma}{2}, \tag{A 14 b}$$

$$u_2=\sin\frac{\beta}{2}\cos\frac{\alpha-\gamma}{2}, \tag{A 14 c}$$

$$u_3=\cos\frac{\beta}{2}\sin\frac{\alpha+\gamma}{2}. \tag{A 14 d}$$

The rank $\frac{1}{2}$ representation Wigner rotation matrix takes the explicit form

$$\left.\begin{aligned} D^{1/2}{}_{1/2,1/2}&=u_0-iu_3, \quad D^{1/2}{}_{1/2,-1/2}=-(u_2+iu_1),\\ D^{1/2}{}_{-1/2,1/2}&=u_2-iu_1, \quad D^{1/2}{}_{-1/2,-1/2}=u_0+iu_3. \end{aligned}\right\} \tag{A 15}$$

We can now couple $\mathbf{D}^{1/2}$ to obtain $\mathbf{D}^1$ in terms of quaternions,

$$D_{m,n}{}^1=\sum C(\tfrac{1}{2}\tfrac{1}{2}1\ ;\ q,\ m-q)C(\tfrac{1}{2}\tfrac{1}{2}1\ ;\ p,\ n-p)D_{q,p}{}^{1/2}\,D^{1/2}{}_{m-q,n-p}. \tag{A 16}$$

We find

$$\left.\begin{aligned} D_{11}{}^1&=(u_0{}^2-u_3{}^2-2iu_0u_3), \quad D_{10}{}^1=-\sqrt{2}(u_0u_2+u_1u_3-iu_2u_3+iu_0u_1),\\ &\qquad\qquad D_{1-1}{}^1=(u_2{}^2-u_1{}^2+2iu_1u_2),\\ D_{01}{}^1&=\sqrt{2}(u_0u_2-u_1u_3-iu_2u_3-iu_0u_1), \quad D_{00}{}^1=(u_0{}^2+u_3{}^2-u_2{}^2-u_1{}^2),\\ &\qquad\qquad D_{0-1}{}^1=-\sqrt{2}(u_0u_2-u_1u_3+iu_2u_3+iu_0u_1),\\ D_{-11}{}^1&=(u_2{}^2-u_1{}^2-2iu_1u_2), \quad D_{-10}{}^1=\sqrt{2}(u_0u_2+u_1u_3+iu_2u_3-iu_0u_1),\\ &\qquad\qquad D_{-1-1}{}^1=(u_0{}^2-u_3{}^2+2iu_0u_3). \end{aligned}\right\} \tag{A 17}$$

Taking the transpose of $\mathbf{D}^1$ and transforming from the spherical to the cartesian representation we can also determine the explicit form for the cartesian rotation matrix $\mathbf{M}(\alpha\beta\gamma)$ connecting a vector $\mathbf{v}$ in the rotated (primed) and original frame

$$\mathbf{v}'=\mathbf{M}(\alpha\beta\gamma)\mathbf{v}. \tag{A 18}$$

The matrix is

$$\begin{pmatrix} (u_0^2-u_3^2+u_1^2-u_2^2) & 2(u_0u_3+u_1u_2) & -2(u_0u_2-u_1u_3) \\ 2(u_1u_2-u_0u_3) & (u_0^2-u_3^2+u_2^2-u_1^2) & 2(u_0u_1+u_2u_3) \\ 2(u_0u_2+u_1u_3) & -2(u_0u_1-u_2u_3) & (u_0^2+u_3^2-u_1^2-u_2^2) \end{pmatrix}. \quad \text{(A 19)}$$

An explicit form for higher rank Wigner rotation matrices in terms of quaternions can be obtained by repeatedly coupling $\mathbf{D}^1$ using the Clebsch–Gordan series.

References

[1] (a) Barker, J. A., and Henderson, D., 1976, *Rev. mod. Phys.*, **48,** 587. (b) Ailawadi, N. K., 1980, *Phys. Rep.*, **57,** 241.

[2] Hansen, J. P., and McDonald, D., 1976, *Theory of Simple Liquids* (Academic Press).

[3] (a) Lasher, G., 1972, *Phys. Rev.* A, **5,** 1530. (b) Lebwohl, P. A., and Lasher, G., 1972, *Phys. Rev.* A, **6,** 426.

[4] (a) Meirovitch, H., 1976, *Chem. Phys.*, **21,** 251. (b) Jansen, H. J. F., Vertogen, G., and Ypma, J. G. J., 1977, *Molec. Crystals liq. Crystals*, **38,** 87.

[5] Zannoni, C., 1979, *The Molecular Physics of Liquid Crystals*, edited by G. R. Luckhurst and G. W. Gray (Academic Press), Chap. 9.

[6] (a) Denham, J. Y., Luckhurst, G. R., Zannoni, C., and Lewis, J., 1980, *Molec. Crystals liq. Crystals*, **60,** 185. (b) Luckhurst, G. R., and Romano, S., 1980, *Molec. Phys.*, **40,** 129. (c) Luckhurst, G. R., and Romano, S., 1980, *Proc. R. Soc.* A, **373,** 111.

[7] Kushick, J., and Berne, B. J., (a) 1973, *J. chem. Phys.*, **59,** 4486. (b) 1976, *J. chem. Phys.*, **64,** 1362. (c) 1977, *Modern Theoretical Chemistry, VB*, edited by B. J. Berne (Plenum Press).

[8] Tsykalo, A. L., and Bagmet, A. D., (a) 1976, *Russ. J. phys. Chem.*, **50,** 439. (b) 1978, *Molec. Crystals liq. Crystals*, **46,** 111. (c) 1978, *Czech. J. Phys.* B, **28,** 1113.

[9] Cf., for example, Chandrasekhar, S., 1977, *Liquid Crystals* (Cambridge University Press).

[10] Zannoni, C., *The Molecular Physics of Liquid Crystals*, edited by G. R. Luckhurst and G. W. Gray (Academic Press), Chap. 3.

[11] (a) Ypma, J. G. J., and Vertogen, G., 1976, *Solid St. Commun.*, **18,** 475. (b) 1976, *J., Phys., Paris*, **37,** 557. (c) Sheng, P., and Woitowicz, P. J.,1976, *Phys. Rev.* A, **14,** 1883. (d) Madhusudana, N. V., Savithramma, K. L., and Chandrasekhar, S., 1977, *Pramana*, **8,** 22. (e) Faber, T., 1980, *Proc. R. Soc.* A, **370,** 509.

[12] Rose, M. E., 1957, *Elementary Theory of Angular Momentum* (Wiley).

[13] Barojas, J., Levesque, D., and Quentrec, B., 1973, *Phys. Rev.* A, **7,** 1092.

[14] (a) Evans, D. J., 1977, *Molec. Phys.*, **34,** 317. (b) Evans, D. J., and Murad, S., 1977, *Molec. Phys.*, **34,** 326.

[15] Cf., for example, Killingbeck, J., and Cole, G. H. A., 1971, *Mathematical Techniques and Physical Applications* (Academic Press).

[16] Zannoni, C., 1979, *Molec. Phys.*, **38,** 1813.

[17] (a) Nordio, P. L., and Busolin, P., 1971, *J. chem. Phys.*, **55,** 5485. (b) Nordio, P. L., Rigatti, G., and Segre, U., 1972, *J. chem. Phys.*, **56,** 2117. (c) Nordio, P. L., and Segre, U., 1975, *Chem. Phys.*, **11,** 57.

[18] (a) Cukier, R. I., 1974, *J. chem. Phys.*, **60,** 734. (b) Lakatos-Linderberg, K., and Cukier, R. I., 1975, *J. chem. Phys.*, **62,** 3271.

[19] (a) Polnaszek, C. F., and Freed, J. H., 1975, *J. phys. Chem.*, **79,** 2283. (b) Huang, L. P., and Freed, J. H., 1975, *J. chem. Phys.*, **63,** 118.

[20] Scott, J. T., 1979, *Physics today*, **31,** 46.

[21] (a) Corda, E., Ronchi, M. E., Guerra, M., Pasini, P., and Zannoni, C., 1979, *Eurographics*, 373. (b) Morettini, L., Stremmenos, C., and Zannoni, C., 1979, *Liquid Crystals*, film directed by L. Morettini, Rep. Cinem. Sci., CNR.

[22] Joly, C. J., 1905, *A Manual of Quaternions* (Macmillan).